

Approaches to plasma desorption mass spectrometry by some theoretical physics concepts¹

E.R. Hilf

Fachbereich Physik, Carl von Ossietzky Universität, D-2900 Oldenburg, Germany

(Received 30 November 1992; accepted 23 January 1993)

Abstract

This report is a collection of some aspects of the work pursued by the theoretical physics group at the University of Oldenburg studying the mechanism of the PDMS desorption process. Specifically we present first a quantitative macroscopic hydrodynamic model designed to describe the PDMS desorption process up to the actual disruption starting from a Lagrangian-density formalism. The microscopic mechanical details of the process are followed by a molecular dynamics program making use of a novel momentum reflection-free boundary condition. Finally we report briefly on the large-scale calculations necessary to calculate the intricate thermal quantum-mechanical properties of clusters, necessary to understand the post-desorption phenomena of desorbed clusters. In the last section we give information on first experiences with computer package tools developed for analyzing PDMS spectra. We hope that these will be widely used by experimentalists for individually analyzing tasks of their own.

Key words: Plasma desorption mass spectrometry; Molecular dynamics; Macroscopic modeling; Microscopic modeling; Cluster production; Cluster degradation.

1. Introduction

1.1. PDMS

Plasma Desorption Mass Spectrometry (PDMS) is a unique method, introduced by Torgerson and Macfarlane and co-workers [1,2], to desorb, ionize and detect molecules and their fragments induced by bombarding a fast heavy ion (in this case fission fragments of ²⁵²Cf) on a surface of a piece of condensed matter (solid or liquid).

The basic process is thoroughly understood [3]: an impinging heavy ion with about the average velocity of the electrons in the solid (“Bohr velocity”) causes a resonant electronic energy transfer

(electronic stopping). In the infratrack, about 40 electrons per Ångström are set free. This dense interacting energetic electron cloud, together with faster δ -electrons, radially enters the cylindrically-symmetric cold surrounding solid. By resonant scattering between each other (because of their similar velocity) they start to form an interacting coherent expanding thermal electron cloud, which, by expansion and then cooling, comes into increasing contact with the electrons of the solid. The most effective way of then transporting electronic energy over larger distances in the solid is by excitons (coupling the passing-by slowing-down electron to an electron hole in the solid) being charge-neutral [4]. Their final trapping and de-excitation gives initial energy to the mechanical system of coupled atoms and molecules of the solid. This is reflected in the fact that solids, for which the

¹ Paper presented at the 6th Texas Symposium on Mass Spectrometry, Gaspé, Que., Canada, 15–19 June, 1992.

excitons de-excite non-phononically, give especially good results with PDMS [5]. The successive release of mechanical energy leads to a shock which finally blasts off up to 10^4 particles, the few of which that are charged are detected and accumulated.

The resulting PDMS mass spectra are rich sources of information on the process, the use of which is still being obscured by the ill-studied and ill-understood subsequent ionization which selects through its own bias only about 0.1% of the particles for experimental detection.

Here we restrict ourselves to contributing some aspects to the understanding of the underlying physical processes involved in PDMS by reporting on some work aimed at gaining a more quantitative picture. Our motive for working in this field is that we hope that because of the complex underlying physical processes, PDMS will, once the mechanisms have been more quantitatively understood, finally emerge as a unique tool for giving information on such diverse fields as solid state physics of fast energetic processes, dense energetic electron showers in solids, large molecular systems in far-off-equilibrium motion, coupling of excitons to phonons, transverse to longitudinal phonons, ionization in a highly excited breaking-up solid, cluster degradation after desorption, or even cluster formation in a supersonic expansion [6].

1.2. Outline

In section 2 we report on a macroscopic hydrodynamic model developed within our group by Barth [15], in which a nonlinear Lagrangian density is designed to allow for a coupling of the radial longitudinal sound shock to the transverse surface oscillation modes, which initiates a static surface-soliton if the energy transfer is sufficiently large. The subsequent desorption and sequential breakup should lead to the PDMS mass yield.

The second paragraph of this section considers what molecular dynamics can do for the understanding of such violent processes; in the third paragraph some analytical tools are described which seem to be needed to extract the maximum

information from actual experimental measurements of PDMS time bin channel spectra.

A large molecular dynamics computer program (CLIMPACT) (see section 3) has been written [7,8] by my co-workers B. Nitzschmann and K. Barghorn, simulating the mechanical reaction of the solid to the primary energy deposition. Up to 10^6 atoms in their coupled Newtonian motion are tracked. The desorbed particles recorded are compared with experimental data. The formation and subsequent incomplete sequential degradation of clusters have been found to be especially sensitive to the details of the process.

The thermal properties of the desorbed clusters determine their subsequent degradation. For loosely bound van der Waals clusters quantum-mechanical effects such as isomerism and zero-temperature kinetic energy become especially important. These have been accessed by Feynman's path integral Monte Carlo method for clusters for $N < 100$ (see section 4). Work is being done in our group by Borsmann for clusters as large as 56 atoms [9–11] using a program called PIMC II.

Software tools for analyzing PDMS spectra have been developed in our group by Curdes and co-workers [26,28,31] to help experimentalists analyzing PDMS spectra. These are presented in section 5. The program PEAKS quickly and automatically extracts the original time bin channel spectrum for properties of mass peaks such as position, content, width, symmetry, etc. The program CRUNCHER is used to calculate the predicted PDMS spectrum for a given structure of a molecule by entropically breaking each chemical bond independently. The bond break-up probabilities are fitted to experimental spectra. Results are given for the rich cluster spectrum of a metal complex salt [31].

1.3. Entropic processes

The type of desorption process met in PDMS is just one of a rather common and large class of violent mechanical processes which we will call entropic desorption.

These are characteristic of a rapid intake of

excess energy in a time short compared with any of the equilibration times of internal systems of degrees of freedom, of enough transfer of energy to internal mechanical stress, still in times short compared with any other relaxation mechanisms, and of release of stress by a large subsequent mechanical collective violent motion leading to the eventual break-up of the desorbed particles. This may be viewed as a coupling of internal macroscopic mechanical degrees of freedom (such as longitudinal sound) to surface transverse modes up to a level where these break up by exceeding the mechanical stress tolerance. This nonlinear coupling of different modes has been called mode scrambling [13] and has not yet been too deeply studied in other fields.

Some typical examples of entropic desorption in other fields of physics are:

(i) nuclear fragmentation after collision with a heavy ion with energy above the Fermi-level: the desorption times are short compared with the nuclear equilibration times;

(ii) electrospray mass spectrometry: the longitudinal flow pulse is coupled to the transverse oscillations leading to droplets in times short compared with thermal or hydro-dynamic equilibrium times;

(iii) the surf at the beach of the St. Laurentian Gulf with its coupling of transverse surface waves to the beach (shallow water as the potential) in times short compared with the hydrodynamic equilibration times.

The desorbed particles involved are quite different, as are the corresponding energies and sizes involved, but in relation to their respective entropic scale they are, in fact, very similar.

The discovery of PDMS with its easy reproducibility and detailed experimental measurements has opened the possibility of a detailed theoretical analysis. Developing methods for modeling the mechanical aspects of PDMS could prove useful in widely differing fields.

2. Macroscopic modeling

Macroscopic models, such as the hydrodynamic

model presented here, are designed to model the basic overall features of the process as a guide for more detailed microscopic simulations. However, the hydrodynamic equations of motion for the large amplitude motions in question here are rather complicated and not well known. Thus, an alternative approach has been chosen: we start from a Lagrangian density L , the terms of which are designed to yield the desired equations of motion by the usual derivatives. The advantage of this approach is that Lagrangians have a simple structure with additive terms for the different contributions to the interaction even for complicated types of motion.

For modeling the first part of the PDMS desorption process we couple the longitudinal phonons to the transverse surface sound field η . In addition, for the surface field, we assume a self-coupling for large amplitudes. Since we are only interested in the build-up of the surface transverse motion, we can even treat the initial longitudinal shock implicitly, keeping only the coupling terms between both field types but neglecting the terms dependent on the longitudinal field alone, such as the kinetic energy and mass or even self-coupling terms. Thus, we choose the Lagrangian [14,15]

$$L(\eta, \partial_t \eta) = \frac{1}{2} (\partial_t \eta)^2 - \alpha \eta^2 + \beta \eta^4 \quad (1)$$

where η is the transverse elevation of the surface and α and β depend on the initiating longitudinal sound-wave amplitude. The terms of L are interpreted as kinetic energy, mass, and a self-coupling term, respectively. This is a typical solitary wave differential equation for η . It may be integrated to

$$\eta(r) = \left(\frac{2\alpha}{\beta} \right)^{\frac{1}{2}} \operatorname{sech}(\sqrt{\alpha} r) \quad (2)$$

In three dimensions the soliton is radially symmetric, the shape of the surface is shown in Fig. 1, with the initiating heavy ion track in the middle of the soliton.

The behavior of the solid in the z direction is approximated by [16]

$$f(z) = \frac{\sinh l(z+d)}{\cosh(ld)} \quad (3)$$

and shown in Fig. 2.

surface deformation

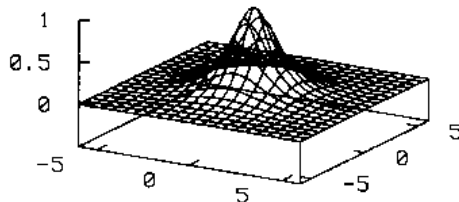


Fig. 1. Surface-soliton being initiated by a fast heavy ion.

A critical curvature κ is introduced as a condition for break-up of the solid. Whenever this critical curvature is reached the solid is assumed to crack up and the material broken loose is then assumed to be subsequently desorbed. Thus, the cracking of a layer is assumed to occur whenever the curvature fulfills the condition

$$\partial_{rr}\eta(r, z) = \frac{2\alpha^2(R^2 - 2)}{\beta R^3} \frac{\sinh l(z + d)}{\cosh(ld)} = \kappa \quad (4)$$

with

$$R = \cosh \sqrt{\alpha r}$$

The shape of the crater is obtained by solving for z with the result

$$z(r, \kappa) = \frac{1}{l} \operatorname{arcsinh} \left[\frac{\kappa R^3 \beta \cosh(ld)}{2\alpha^2 R^2 - 4\alpha^2} \right] - d \quad (5)$$

The form of the crater is shown in Fig. 3, the parameters for the depth are $d = 10$, for $\alpha = \beta = 1$ and for the curvature $\kappa = -0.1$.

The total amount of the desorbed material, assumed to be the volume of the crater, can then

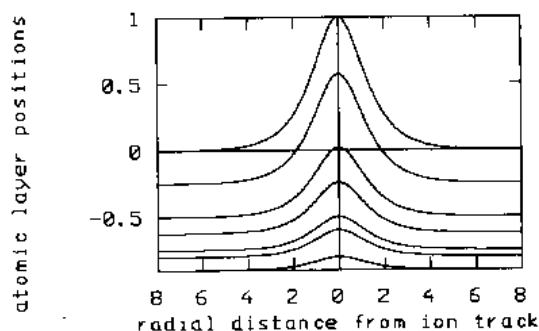


Fig. 2. Non-propagating soliton-type distortion of the surface layers of a solid some picoseconds after the initial heavy ion impact.

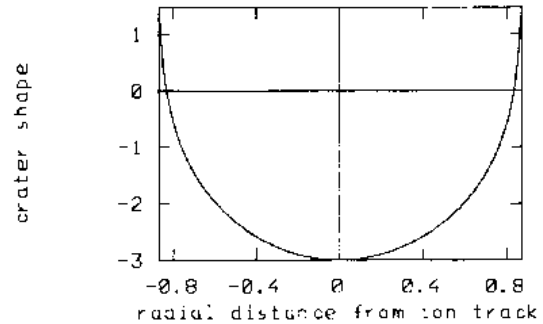


Fig. 3. Crater from the crack-condition of maximal local stress.

be calculated by

$$V = \pi \int_0^{r(0, \kappa)} [r(z, \kappa)]^2 dz \quad (6)$$

At the moment we are studying the dependence of the amount of material desorbed and its kinetic energies on the solid-state properties of the solid.

3. Microscopic simulation by molecular dynamics

3.1. Simulations

The details of the initiated far-off stability motion of the atoms of the target after the initial stimulation by the electronic excitation can be simulated by solving the Newtonian coupled equations of motion for all particles involved in the solid. First molecular dynamics calculations were undertaken in 1987 [17] for two-dimensions in space, and just vertical velocity direction and a small number of particles (some 300). However, with the desorption of 10^4 particles the chunk of the solid to be simulated should be much larger. Generalizing to the initial impact not only of ions but also of clusters of atoms, a cluster impact molecular dynamics computer program CLIMPACT has been set up [7,8] and is being applied by my co-workers B. Nitzschmann and K. Barghorn. The desorbed particles recorded are compared with experimental data. The formation and subsequent incomplete sequential degradation of clusters have been found to be especially sensitive to the details of the process. Specifically, three-dimensional simulations of up to 10^5 particles can be supported.

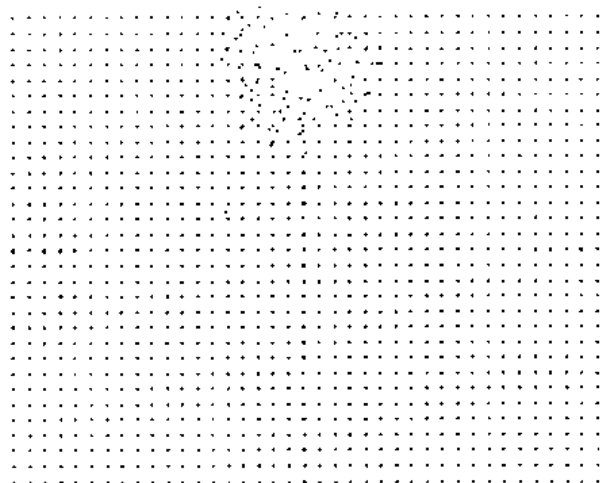


Fig. 4. Three-dimensional MD-simulation: impact of Au on an Au target 0.081 ps after impact. Shown is a projected central two-dimensional slice.

The atoms of the solid are assumed to form initially a cubic monocrystal target with fcc structure bound by the usual Lennard-Jones potential. When hitting the target, some projectile particles are reflected and others penetrate, but both together initiate a shockwave which propagates toward the target boundary. In Figs. 4–7 we show some snapshots of such a simulation for the case of a slow gold ion (1 keV u^{-1})

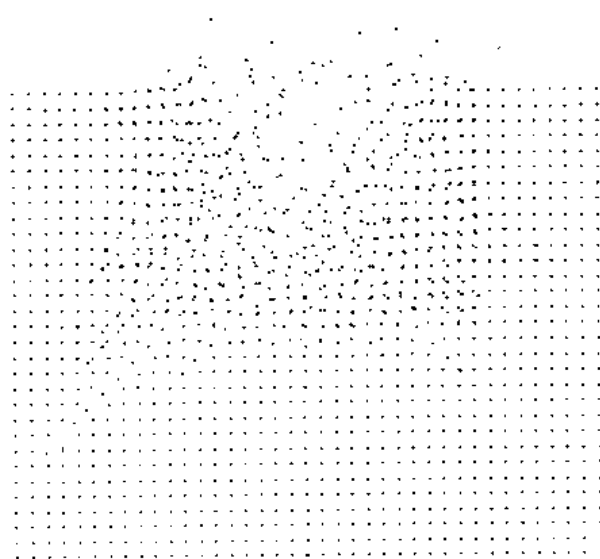


Fig. 5. MD-simulation: impact of Au on an Au target 0.330 ps after impact.

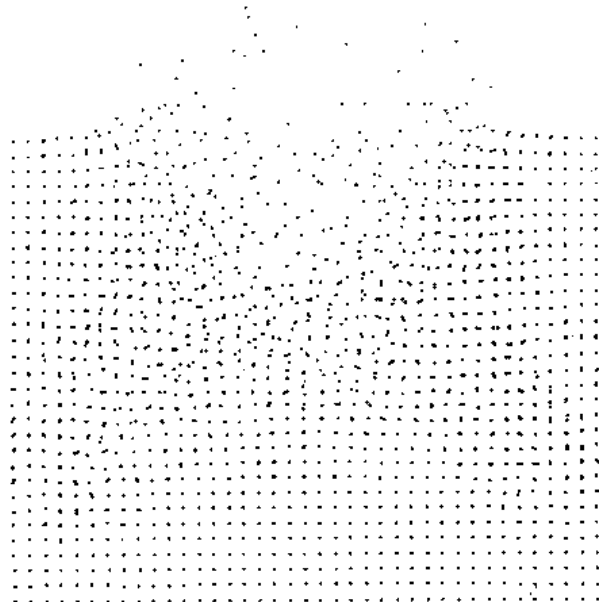


Fig. 6. MD simulation: impact of Au on an Au-target 0.750 ps after impact.

shot on a gold target, simulated by a large array of ($16 \times 20 \times 20 \text{ fcc} = 25.600$) atoms for four time steps. In Fig. 7 the initiated soundwave reaches the surface of the simulated target piece. The crater shape being formed resembles the

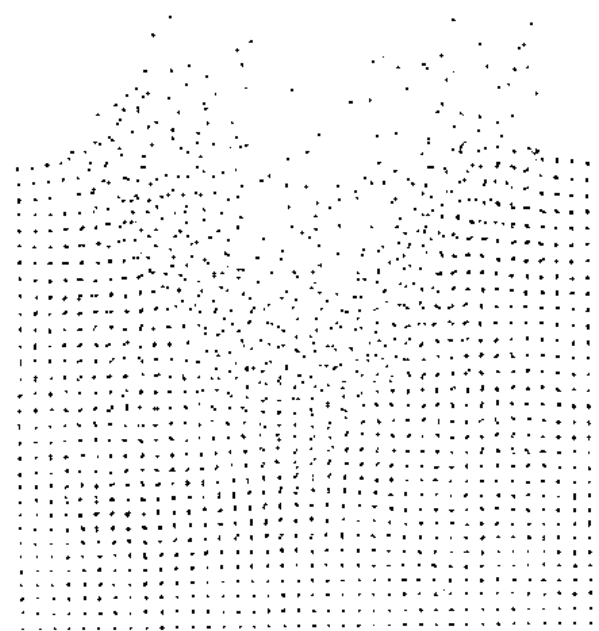


Fig. 7. MD simulation: impact of Au on an Au-target 1.561 ps after impact.

one calculated by the macroscopic model in section 2. The final crater is expected, however, to be much shallower owing to post-desorption annealing.

At the moment, the sputtering behavior dependent on impact angle, projectile size and impact energy is being studied. Furthermore, we are studying the dependence on electronic effects using an ansatz of Kammer and Hilf [3,4] for the interatomic potential of excited atoms. CLIMPACT is now already being applied on a routine basis.

3.2. Non-local boundary condition

Boundary conditions at the side of the piece of matter (which is assumed to be homogenous) should, for example, for MD calculations, simulate that the piece is just a part of an extended homogenous solid. Thus, for example, a shock-wave should not be reflected at the boundary of the lattice piece chosen. However, the currently used boundary conditions [18–20] are either periodic or reflecting; both reflect momentum which then disturbs the process. It can be proven that this holds true for any definition of a local boundary condition, including the one proposed [21] to increase the mass of the “surface” atoms or any combinations of these. For a detailed discussion of boundary conditions see ref. 13.

To minimize the unwanted effect of momentum reflection at the interior boundary we thus propose a non-local boundary condition. An easy-to-use method has been tested [22]: for the last three layers of atoms at the interior boundaries we introduce an additional friction force $\vec{f} = -\alpha\vec{v}^2$. α is determined by minimizing the momentum reflection at the surface. Such an “artificial viscosity” is known, for example, from the shockwave calculations in the simulation of supernova explosions in astrophysics [23] as in many other fields. For the numerical solution of nonlinear equations, the space coordinates have to be discretized. The artificial friction extracts the momentum and energy at the surfaces of the simulated piece of matter which

in reality would be proceeding safely out of the piece into the surrounding solid owing to the homogeneity of the material.

4. Thermal quantum-mechanics of clusters

4.1. The PIMC II program

PIMC II is a computer program developed by Franke et al. [11] to investigate thermal properties of small clusters ($N < 100$) via the path integral Monte Carlo method. The thermal properties of clusters such as pair correlation function, specific heat, and potential or kinetic energy are calculated quantum-mechanically for Fermi–Bose and Boltzmann quantum statistics as well as for classical Maxwell statistics. The program is highly vectorized and uses very efficient algorithms. PIMC II runs 20 to 120 times faster than PIMC I [9,10], which includes solely Boltzmann statistics.

4.2. Applications

Denoting the binding energy of Neon clusters [11] for a temperature T with E_n , the second energy differences $\Delta^2 E_n = E_{n-1} + E_{n+1} - 2E_n$ have proved to be a good measure for cluster stability [33]. If $\Delta^2 E_n$ is positive, the process of fragmentation of an Ne_n cluster into an Ne_{n-1} cluster and a single Ne atom is less favorable than the process of fragmentation of an Ne_{n-1} cluster into an Ne_n cluster and a single Ne atom, i.e. positive values indicate high stability of Ne_n clusters and thereby magic numbers. The result is that only with these quantum mechanical calculations are experimentally known magic numbers reproduced, thus emphasizing the importance of the quantum statistics for the stability of low-mass atomic clusters.

The pair correlation function gives the distribution of distances between the atoms of a cluster. For Ne_{13} clusters at 4.0 K the quantum kinetic energy increases the two-particle distances and broadens the distribution compared with the classical calculation. At 8.0 K the

structure gets washed out and the clusters seem to become fluid like.

First results for ^3He -clusters were presented at the ISSPIC 1992 conference [24]. Simulations for Li and molecular clusters are in progress.

The clusters desorbed by PDMS are probably excited. Their degradation will be governed by their quantum-mechanical properties, which we are studying at the moment.

5. Computer analysis tools for PDMS spectra

Computer analysis tools have been developed for evaluating PDMS spectra. These include algorithms for efficient data reduction, algebraic tools, and a program for the simulation of the fragmentation process.

5.1. PEAK evaluation

PEAKS is a program [25,26] which extracts relevant mass line data such as amplitude, area, width and asymmetry of relevant peaks in channel spectra, by a new method, the far moments, in a very efficient way. The spectrum is scanned just once (with no fit of, for example, Gaussians) to extract the experimental lines. The new algorithm only calculates one set of sums (typically 3-4) of differently weighted channel contents over a region of about one line width, starting well to the left of an expected line. This procedure is extremely fast and works as well for noisy spectra and asymmetric line shapes. It can and has been automated. The program package is available on request from the authors.

Results demonstrate the high sensitivity for extracting even small lines out of a large background noise with no fit.

The efficient algorithm allows the processing of huge amounts of data (typically 220 kilobytes per spectrum) on a 286 PC in a competitive time. Further development and research is being done to identify noise and to subtract these from the original spectrum automatically.

5.2. CRUNCHER

Some of the basic tasks to analyze PDMS spectra are:

(i) to determine the atomic weight of the molecule of a chemically "pure" sample;

(ii) to determine the chemical structure of a chemically pure substance;

(iii) to determine the composition of a given mixture of substances;

(iv) to determine to which class of a given set of classes a given sample's material belongs without being interested in what may be rather complex or unknown chemical composition.

The first task is the easiest one to deal with. Thus, calibration and isotopic deconvolution are routine.

For the second task, tools have been developed to help the experienced experimentalist. For molecules of linear chemical structure many tools are available to automate the "mass-sum" hunting: if the sum of two masses is equal to the mass of the molecule, the two are assumed to be atoms (building blocks) linked by a chemical bond. By noting all bonds even large polypeptides have been routinely sequenced [27].

For molecules with a more complex chemical structure (e.g. rings or bridges) more elaborate tools are necessary.

We have developed two software tools, SYNTH and CRUNCHER (see Figs. 9 and 10 for an example), to be used together. This program [25,26] calculates the composition of a theoretical PDMS spectrum by assuming the chemical bond break-up probabilities for a molecule of known chemical structure to be independent of each other. This reflects the rather rapid (as compared with bond vibration times) entropic deposition of a large amount of energy as thought to occur in the PDMS process. The bond break-up probabilities are fitted to experimental spectra by using a linear scalar product measure. The breaking algorithm has been given in ref. 25. Curdes and Hilf [31] introduced, for these highly non-linear functions, a method of fits in the multi-dimensional parameter space, a

Monte Carlo start combined with an attached local minimum search. This proved the optimal case of many side minima. As an example we studied a four parameter fit for the bonds of the carbon backbone of the hydrocarbon nonane [6]. Thus, a symmetric distribution of four different bond strengths is assumed. The first 486 runs of CRUNCHER which the program chose gave already a good determination of the best set of the four bond strengths. In Fig. 8 we show the quality of the fit for one of the four parameters, the innermost bond pair in the chain. Clearly, the program specifically explores the envelope of the distribution, instead of a random approach. The aim is to obtain values for the break-up probabilities for certain bond types such as C–H, C–C etc. (which should be about the same for different substances) which are then to be explained by quantum-mechanical calculations. In this way we hope to elucidate the mechanism which governs this fragmentation process and to enlarge the quality of the predictions made by CRUNCHER.

5.3. Synthesis program

With SYNTH we first scan the experimental spectrum for all possible bonds, thus creating a bond-list. This may be called a three mass line rule. The next step is then to scan this for pairs of bonds with

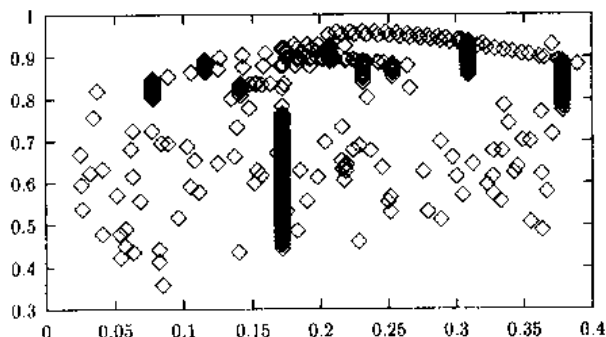


Fig. 8. Similarity between the experimental PDMS spectrum of nonane [6] and predictions by the program CRUNCHER as a function of the bond break-up probabilities. Shown is the distribution for the innermost bond break-up probability for only 486 runs in this four-dimensional parameter-space run. Clearly, the program CRUFIT of ref. 31 explores specifically the area of the maximum.

a common fragment but with the absence of a bond for the two disjunct fragments of the two bonds [25]. This is a seven mass line rule. Together with a cluster-scan program, giving all series of clusters with their integrated intensity, starting mass, "atomic" mass (cluster mass), and the number of successive cluster sizes, these tools proved practical for extracting information on the chemical structure.

5.4. Similarity measures

In mass spectrometry a standard task is to invent a measure for the similarity of one spectrum to another. The idea is that if a spectrum is similar in that respect to another given one, then these two might be of similar chemical composition. This is especially useful for quality control in the pharmaceutical industry, or for identifying the oil type from a sample taken from an oil spill [32].

For the usual mass spectra of, say, electron impact some 10 dominant lines of the spectrum are depicted. This set of masses is then seen as a vector of 10 components in a vector space called the spectrum space \mathcal{H} which is a linear vector space with as many dimensions as possible masses in the spectrum. For this Hilbert space of finite dimension d (say, $d = 100$), a Euclidean metric is introduced, allowing a similarity measure to use the inner product of two spectra Y_1, Y_e given by $(Y_1, Y_e) = \sum_{i=1}^d Y_1 Y_e$ which is also used for defining "distances" between spectra. In Hilbert space the similarity of a spectrum with itself is an important observation, its square root being the length of the vector. This is the important invariant of a spectrum, and should be independent of coordinate transformations. Because of the widespread knowledge of Linear Algebra this approach to mass spectra has been widely adopted.

However, this strategy has several disadvantages. The only important number for a spectrum by summing all mass lines is the total number of counts, not the sum of their squares. Thus an algebraic solution, suited and designed for treating

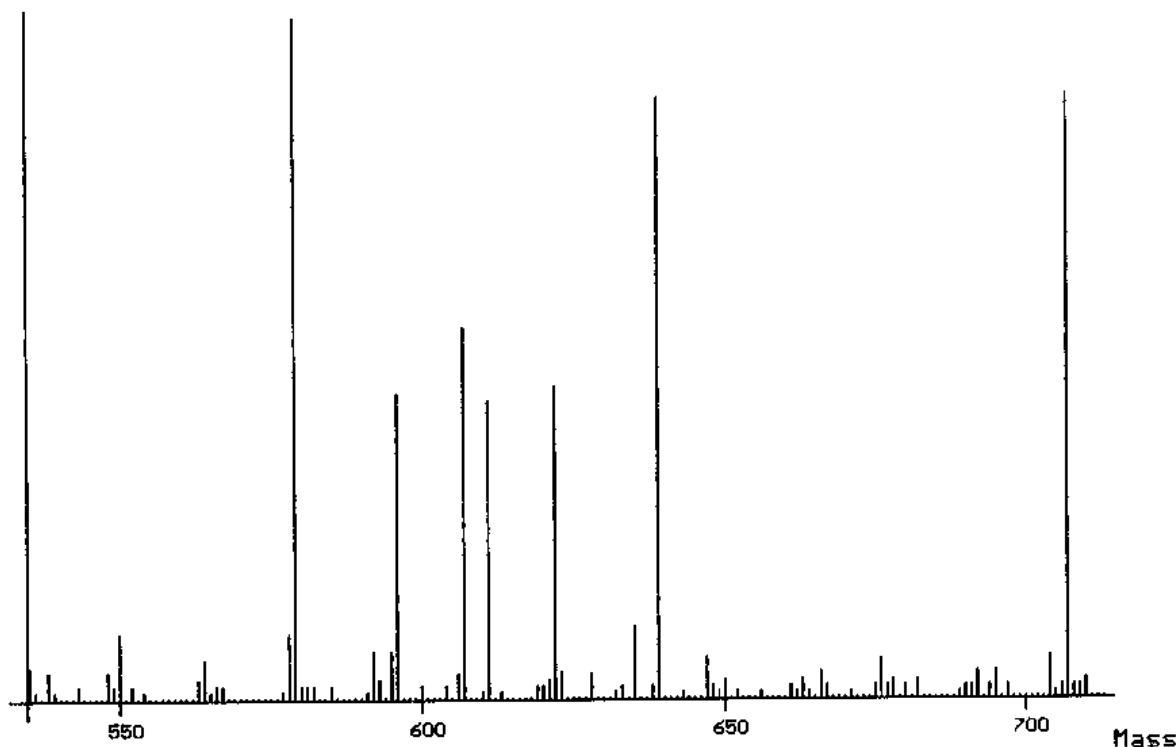


Fig. 9. Result of CRUNCHER for an independent bond break-up simulation for the substance *P*, not fitted to experimental data (part of the predicted spectrum).

mass spectra, should give as the length of the spectrum the total number of counts:

$$[Y_1, Y_1] = \sum_{i=1}^d Y_1(m_i) \quad (7)$$

Thus, to generalize this to the definition of an inner product, we gain the desired respectively constructed linear similarity measure for two spectra by

$$[Y_1, Y_e] = \frac{\sum_{i=1}^d \sqrt{(Y_1, Y_e)}}{\sqrt{[\sum Y_1(i) \sum Y_e(i)]}} \quad (8)$$

This measure is linear in the difference between each mass line yield, as one should expect for a similarity measure. In contrast, the Euclidean measure gives a quadratic dependence, suppressing slight amplitude differences for the same mass in the different spectra. This can be proved simply by assuming all yields of each spectrum to be

different by a constant additive δ . Then the Euclidean similarity measure varies as δ^2 while the linear one varies as δ , as desired in mass spectrometry. Both, however, have the same linear dependence on the averaged square of the deviation if all spectra would be normalized to the same number of counts.

The price of a loss of linearity of the resulting algebra is not relevant here since coordinate transformations are not applicable anyhow, since linear combinations of masses have no physical meaning. Instead, each mass contains independent chemical information. Thus the only "coordinate system" needed is the one given, each mass unit is one coordinate.

An additional advantage of this strategy is that no *differences* of masses or yields occur, which might, by Hilbert-space linear coordinate transformations, turn out to be negative. Here, as in real experimental mass spectra, no negative masses or negative yields ever occur or

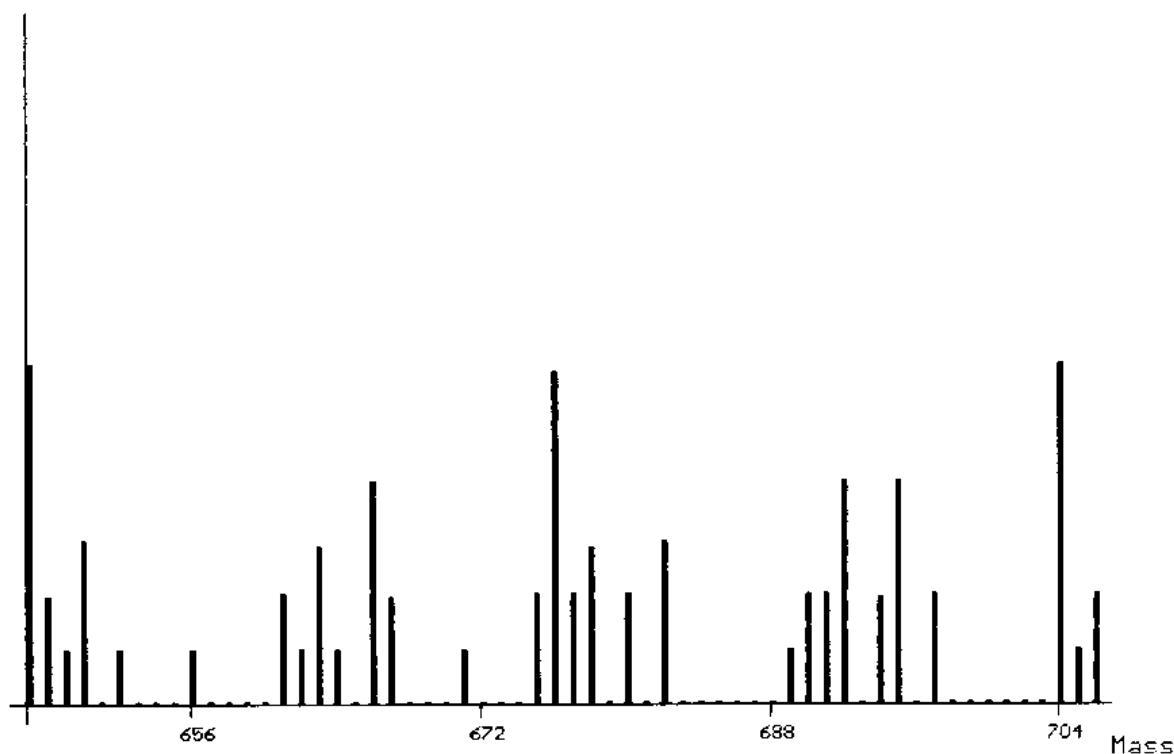


Fig. 10. Prediction of PDMS spectrum for substance *P*. Result of CRUNCHER independent bond break-up simulation for the substance *P*. This blow-up of Fig. 9 shows contributions for fragments gained by 2–6 simultaneous bond break-ups.

have to be dealt with in the process of the algebraic rules.

5.5. Problems of large spectra

PDMS, because of the often conspicuous molecular peak, can be also applied to analyze rich compounds, such as sediments, e.g. from the Wadden Sea [30], oils [32], lignins, humin and gelbstoff materials. For their spectra, of very many relevant mass lines, we use the name “large spectra”. For these, the usual strategy of defining a similarity measure becomes more problematic the larger the number of mass lines. The reason for this is that, for the above mentioned similarity measures, all the numerous relevant masses contribute. In other words, two chemically similar spectra, if they contain very many relevant mass lines, might appear pretty dissimilar in terms of the above defined measures, or vice versa, owing to the

large number of sum terms with their individual experimental uncertainties.

This problem is well known in linear algebra of Hilbert spaces. For the limit of infinite dimensions two definitions of convergence of a set of spectra to a given one become different. To be of “weak convergence” the yield of each mass line has to become closer and closer to the respective line of the reference spectrum. To be of “strong convergence”, however, the limit of the inner product between the lines of an element of the set and of the reference one has to go towards zero. In other words, although the spectrum may look more and more similar, owing to the sum over the enormously large number of masses, the integral similarity measure may indicate dissimilarity in using an absolute distance between two spectra as a measure. In the limit of infinite dimensions both strong and weak convergence are not the same.

We thus complement the usefulness of the linear similarity measure by a set of nonlocal but confined

anti-autocorrelation contrast measures as rule-based filters using the same linear inner product (Eq. (8)) prior to applying the comparison. An early version of this idea is given in ref. 29:

$${}_f Y_1 = Y_1(i)(1 - \Gamma) \quad (9)$$

with

$$\Gamma\{Y_1[Y_1(j), j]\} = \frac{[Y_1(i), Y_1(j)]_f^n}{\{[Y_1(i), Y_1(i)]_f^n [Y_1(j), Y_1(j)]_f^n\}} \quad (10)$$

where the sums are taken over $j = i, i \pm 1, i \pm 2, \dots, i \pm n$. For identification of spectra as a member of a class of spectra, or by adapting the definition of such classes by using an adaptive neural network scheme, Eq. (9) becomes, as desired, zero, if $Y_1(i) = Y_1(j) = \text{constant}$ in the mass interval studied — the “ideal” zero-contrast spectrum; in this case the vector $Y_1(i)$ would be omitted. If, however, $Y_1(i)$ is similar but not identical to its neighbors, then the difference in anticorrelation rises quadratically. In the limit of $Y_1(i)$ being very conspicuous over its neighbors, $Y_1(i)$ has the weight $1 - 1/\sqrt{(n)}$, which is equal to unity in the case of a sufficiently large interval. Thus the anti-correlation filter (Eq. (9)) has all the desired properties of a contrast filter.

Interestingly, Γ does not depend explicitly on $Y_1(i)$, instead one obtains the simple relation

$$\Gamma(n) = \frac{1}{\sqrt{(n)}} \frac{\sum \sqrt{Y_1(j)}}{\sqrt{[\sum Y_1(j)]}} \quad (11)$$

6. Acknowledgements

I am extremely thankful to my young and active collaborators, who did most of the work presented here, and who made physics so enjoyable by their creating an active, stimulating, and social atmosphere in the Institute; P. Borrmann, H. Barth, K. Barghorn, B. Curdes, J. Curdes, B. Diekmann and B. Nitzschmann.

Our experimental colleague, W. Tuszynski, was

most helpful in exhibiting new physics by continuous discussions and stimulation.

I enjoyed an elucidating discussion with T.A. Tombrello, when at Gaspé, on the applicability of the Lagrangian method to systems far from equilibrium and with W. Ens on the substance P.

We praise especially C. McNeal, for organizing the PDMS meeting at Gaspé which brought me into contact also with related fields necessary for pursuing our work, and for creating an absolutely stimulating atmosphere.

References

- 1 D.F. Torgerson, R.P. Skowronski and R.D. Macfarlane, *Biochem. Biophys. Res. Commun.*, 60 (1974) 616.
- 2 R.D. Macfarlane and D.F. Torgerson, *Science*, 191 (1976) 920.
- 3 H.F. Kammer. PhD thesis, University of Oldenburg, 1991 (and references cited therein).
- 4 H.F. Kammer and E.R. Hilf, Excitonic processes in F-HIID, in A. Hedin, B.U.R. Sundqvist and A. Benninghoven (Eds.), *Ion Formation from Organic Solids*, Proc. IFOS V, 1989, Wiley, Chichester, 1990, p. 197.
- 5 E.R. Hilf, H.F. Kammer and B. Nitzschmann, Status of the theory of MeV-ion electronic stopping induced desorption, *Radiation Effects and Defects in Solids*, Vol. 110, pp. 89–90.
- 6 E.R. Hilf, W. Tuszynski, B. Curdes, J. Curdes, M. Wagner and K. Wien, *Int. J. Mass Spectrom. Ion Processes*, (1993) in press.
- 7 B. Nitzschmann and K. Barghorn, Molecular dynamics for heavy ion induced desorption, unpublished work.
- 8 B. Nitzschmann, Molekulardynamik für schwerionen-induzierte Desorption. Master's thesis, University of Oldenburg, Germany, 1992.
- 9 G. Franke, E.R. Hilf and L. Polley, *Z. Phys. D*, 9 (1988) 343.
- 10 G. Franke and J. Schulte, Quantum effects and structure of noble-gas clusters, *Z. Phys. D*, 12 (1989) 65.
- 11 G. Franke, E.R. Hilf and P. Borrmann, *J. Chem. Phys.*, 98(4) (1993) 3496.
- 12 W. Tuszynski and R. Angermann, Chlorophyll and other pigments in photoactive and buried marine microbial mats, in W. Tuszynski and E.R. Hilf (Eds.), *Mass Spectrometry of Large, Non-Volatile Molecules for Marine Organic Chemistry*, Int. Workshops on the Physics of Small Systems, Vol. 3, World Scientific, Singapore, 1990, p. 131.
- 13 H.-P. Baltes and E.R. Hilf. *Spectra of Finite Systems*, Bibliographisches Institut Mannheim, Vienna, 1976.
- 14 J. Wu, R. Keolian and I. Rudnick, Observation of a non-propagating hydrodynamic soliton, *Phys. Rev. Lett.*, 52 (1984) 1421.

- 15 H. Barth, Entropische Desorption durch mode scrambling longitudinaler und transversaler Phononen, Master's thesis, University of Oldenburg, Germany, 1992.
- 16 A. Larraza and S. Puttermann, Theory of non-propagating surface-wave solitons. *J. Fluid Mech.*, 148 (1984) 443.
- 17 B. Nitzschmann, E.R. Hilf and H.F. Kammer, Computer simulations of F-HIID, in A. Benninghoven (Ed.), *Mass Spectrometry of Involatile Material*, in *Ion Formation from Organic Solids*, Proc. IFOS IV, 1987, Wiley, Chichester, 1989, p. 97.
- 18 B.J. Garrison, State selected studies of particles desorbed from surfaces by ion beams, *Nucl. Instrum. Methods B*, in press.
- 19 G. Betz and R. Kirchner, Molecular dynamics study of dimer emission from Cu(111) under Ar ion bombardment, in P. Sigmund (Ed.), *Fundamental Processes in Sputtering of Atoms and Molecules*, SPUT 92 Symposium, *Nucl. Instrum. Methods B*, in press.
- 20 M.H. Shapiro and T.A. Tombrello, Molecular dynamics simulations of sputtering involving clusters, *Nucl. Instrum. Methods B*, in press.
- 21 J. Sunner, Phase explosion and ion formation mechanisms, in *Ion Formation from Organic Solids*, Proc. IFOS V, 1989, Wiley, Chichester, 1990.
- 22 B. Nitzschmann and E.R. Hilf, Non-local boundary conditions for molecular dynamics, in preparation.
- 23 F.-K. Thielemann, PhD thesis, Nuclear Astrophysics Group (E.R. Hilf and Dr. W. Hillebrandt), Technische Hochschule Darmstadt, Germany, 1980 (and references cited therein).
- 24 P. Borrmann, Proc. ISSPIC 1992.
- 25 St. Harsdorf and E.R. Hilf, Computer simulations, analysis and transfer of PDMS spectra, in W. Tuszynski and E.R. Hilf (Eds.), *Mass Spectrometry of Large, Non-Volatile Molecules for Marine Organic Chemistry*, *Int. Workshops on the Physics of Small Systems*, Vol. 3, World Scientific, Singapore, 1990, p. 164.
- 26 A. Dullweber, St. Harsdorf, M. Hilf, K. Kruse, W. Schlez, U. Schöle and P. Wagener, PDMS evaluation programs, unpublished work.
- 27 P. Roepstorff, *Nucl. Instrum. Methods*, submitted.
- 28 J. Curdes, P. Borrmann, E.R. Hilf and W. Tuszynski, Computer analysis tools for PDMS spectra, Proc. 40th ASMS Conference on Mass Spectrometry and Allied Topics, Denver, CO, 1992.
- 29 J. Curdes, Studienarbeit, University of Oldenburg, Germany, 1992.
- 30 K. Wien, PDMS applied to frozen marine sediments, in W. Tuszynski and E.R. Hilf (Eds.), *Mass Spectrometry of Large, Non-Volatile Molecules for Marine Organic Chemistry*, *Int. Workshops on the Physics of Small Systems*, Vol. 3, World Scientific, Singapore, 1990, p. 82.
- 31 J. Curdes and E.R. Hilf, Computer analysis tools for PDMS spectra, *Fresenius Z. Anal. Chem.*, 344 (1992) 140.
- 32 J. Curdes and E. Hilf, Identification of Oil types by PDMS, Helgolaender Meeressuntersuchungen, Biologische Anstalt Helgoland, in press.
- 33 V. Bonacić-Koutecký, P. Fantucci and J. Koutecký, *Chem. Rev.*, 91 (1991) 1035.